Fields and propagation characteristics in vacuum of an ultrashort tightly focused radially polarized laser pulse

Yousef I. Salamin
Department of Physics, American University of Sharjah, Post Office Box 26666, Sharjah, United Arab Emirates
(Received 18 August 2015; published 16 November 2015)

Analytic expressions for the electric and magnetic fields of a radially polarized ultrashort and tightly focused laser pulse, propagating in vacuum, are derived from scalar and vector potentials satisfying simple initial conditions. It is shown that for a pulse of axial length comparable to a wavelength, only the zeroth (lowest-order) term in a power-series expansion of the vector potential is needed. A procedure is outlined which may be used to obtain the fields analytically, to any desired order. Most of the needed analytic work is done that would lead to the vector potential from which the fields may be derived and the main expressions are given.

DOI: 10.1103/PhysRevA.92.053836 PACS number(s): 42.65.Re, 52.38.Kd, 37.10.Vz, 52.75.Di

I. INTRODUCTION

There has been a recent surge in interest in radially polarized light, motivated mainly by emerging practical applications [1–3]. Theoretical efforts aimed at appropriately modeling radially polarized laser beams and laser pulses thus continue to appear in the scientific literature [4]. Most applications require low laser intensity and low power [5–8], but the demand for ultrahigh intensities and super powers [9], for such applications as laser acceleration of particles, is also gaining momentum [10–13]. Two special features of laser pulses of the radially polarized variety make them most suitable for specific applications. It has been experimentally demonstrated [14,15] that such pulses may be focused to smaller spot sizes than their linearly polarized counterparts. Radially polarized light has two electric field components, one axial (oscillating along the propagation direction) and one radial (oscillating towards and away from the focus). The radial component vanishes at all axial points, which qualifies it to play a confining role for particles on the beam's direction of propagation, while the other component works to efficiently accelerate the particle axially [16].

Earlier theoretical efforts to model the fields of ultrashort and tightly focused laser light have been based on the so-called Lax series [17,18] and complex-source-point methods [19–22]. Both approaches, however, have their limitations. For example, validity of the Lax series approach is in doubt when used to model the fields of a pulse for which the diffraction angle, defined as $\varepsilon = \lambda/w_0$, approaches unity. In the definition of ε,λ is the laser wavelength and w_0 is the waist radius at focus.

The aim of this paper is to present a systematic derivation of analytic expressions for the electric and magnetic fields of an ultrashort and tightly focused laser pulse, which takes into account explicitly the axial extension of the pulse profile. The approach benefits from one that was advanced twenty years ago by Esarey *et al.* [23] for a linearly polarized pulse, with an important point of departure, namely, the use of vector and scalar potentials instead of just a vector potential. Introduction of the scalar potential results in the fields developing, automatically, axial components in addition to the transverse ones [24]. This method has also been implemented in our recent work [25]. The scalar and vector potentials, linked by the Lorenz gauge condition, satisfy two mathematically similar wave equations which are entirely equivalent to the full set of Maxwell equations in vacuum [26]. A Fourier transform method will be employed to arrive, fully analytically, at the sought vector potential. At some point in the analytic work, a power-series expansion will be used, which renders term-by-term evaluation of the complicated integrals possible.

In Sec. II, solution to the vector potential wave equation will be briefly outlined. This is followed in Sec. III by a simple textbook model for the axial focusing of the pulse. The Fourier transform of the *square function* axial profile leads to a simple definition for the axial pulse extension, to be loosely referred to, henceforth, as the initial *pulse length*. The general analytic work will be presented in Secs. IV and V. Expressions for the leading terms of the electric and magnetic fields, $\boldsymbol{E}$ and $\boldsymbol{B}$, respectively, will be derived in Sec. VI and their main propagation characteristics will be discussed. Our conclusions will be presented in Sec. VII.

II. SOLUTION TO THE WAVE EQUATION

The wave equations satisfied by the scalar and vector potentials follow from the sourceless Maxwell equations, and their solutions are linked by the Lorenz gauge. Starting with a linearly polarized vector potential, say $A_z(x,y,z,t)$, similar dependence upon the space-time coordinates of the scalar potential $\Phi(x,y,z,t)$ will be assumed [24]. The wave equation satisfied by the associated scalar potential is identical to that satisfied by the *only* component of the vector potential. It suffices, therefore, to develop a solution for A_z and then use the gauge condition to determine Φ.

To that end, a change of variables from a set based on the cartesian (x,y,z) is carried out first to the set (ρ,ζ,η), where $\rho = \sqrt{x^2+y^2}/w_0$ with w_0 being the waist radius at focus of the pulse, $\zeta = z - ct$, and $\eta = (z+ct)/2$. For a point within the pulse, moving at the speed of light, the coordinate $\eta = ct$ gives the position of the point at any time relative to the origin of coordinates. On the other hand, $\zeta = 0$ for such a point, which qualifies ζ for serving as a coordinate relative to the *moving* centroid of the pulse. In terms of the new variables, the wave equation for the vector potential reads

$$\left(\frac{1}{\rho}\frac{\partial}{\partial\rho}\rho\frac{\partial}{\partial\rho} + 2w_0^2\frac{\partial^2}{\partial\eta\partial\zeta}\right)\boldsymbol{A} = 0. \tag{1}$$

Solution to the wave equation of the vector potential, which leads to the radially polarized fields, starts with the ansatz [17]

$$\boldsymbol{A} = \hat{z} a_0 a(\rho,\zeta,\eta) e^{ik_0\zeta}, \tag{2}$$

where a_0 is a constant *complex* amplitude and k_0 is some central wave number, which corresponds to a central frequency $\omega_0 = ck_0$. Note that $\boldsymbol{A}$ is polarized axially, i.e., along the propagation direction, which we take as the z axis of a Cartesian coordinate system. Substitution of Eq. (2) into Eq. (1) gives an equation for $a(\rho,\zeta,\eta)$. Then employing the Fourier transform

$$a(\rho,\zeta,\eta) = \frac{1}{\sqrt{2\pi}} \int_{-\infty}^{\infty} a_k(\rho,k,\eta) e^{ik\zeta} dk \tag{3}$$

will turn that equation into

$$\left(\frac{1}{\rho}\frac{\partial}{\partial\rho}\rho\frac{\partial}{\partial\rho} + 4i z_{rk}\frac{\partial}{\partial\eta}\right) a_k = 0 \tag{4}$$

for the Fourier components a_k. In Eq. (4) the quantity $z_{rk} = (k + k_0)w_0^2/2$.

Equation (4) admits the following exact solution, which may readily be verified by direct substitution:

$$a_k(\rho,k,\eta) = \frac{f_k}{1+i\alpha_k} \exp\left[-\frac{\rho^2}{1+i\alpha_k}\right]; \quad \alpha_k = \frac{\eta}{z_{rk}}, \tag{5}$$

in which f_k is an appropriate function of k. With the focus of the pulse taken initially (at $t = 0$) at the origin of the Cartesian coordinate system, its initial position will be at $\eta = 0$ in the new system. From Eq. (5) follows that $a_k(\rho,k,0) = f_k \exp(-\rho^2)$, and Fourier transform of f_k, to be denoted below by $f(\zeta)$, will then serve as an initial axial profile for the pulse emitted at $t = 0$. Effectively, a plausible choice for f_k will yield an appropriate initial axial profile $f(\zeta)$.

III. INITIAL AXIAL PULSE ENVELOPE

Suppose the initial pulse (at $t = 0$) has a narrow band of wave numbers of width Δk centered at some value k_0. This corresponds to the pulse having a frequency bandwidth of $\Delta\omega = c\Delta k$, centered about the frequency $\omega_0 = ck_0$. These features can be exhibited, in a most straightforward way, by the following profile in k space:

$$f_k = \begin{cases} \frac{\sqrt{2\pi}}{\Delta k}, & |k - k_0| \leqslant \frac{\Delta k}{2}; \\ 0, & \text{elsewhere.} \end{cases} \tag{6}$$

Graphically this is a square function of height $\sqrt{2\pi}/\Delta k$ and width Δk. This model will prove to be quite useful in arriving at explicitly analytic field expressions. The corresponding spatial profile (in ζ) may be obtained as the Fourier transform:

$$f(\zeta) = \frac{1}{\sqrt{2\pi}} \int_{-\infty}^{\infty} f_k e^{ik\zeta} dk = e^{ik_0\zeta} \frac{\sin(\zeta\Delta k/2)}{\zeta\Delta k/2}. \tag{7}$$

Since $\zeta = z$, at $t = 0$, it is plausible to take, as the initial pulse length, the quantity $L = \Delta z = \Delta\zeta$. Note that $f(\zeta)$ has zeros at $\zeta\Delta k/2 = \pm N\pi, N = 1,2,\ldots$. This suggests that an appropriate choice for the axial length of the pulse may be $L = \Delta\zeta \sim 2\pi/\Delta k$, which is roughly analogous to the full width at half-maximum of a Gaussian profile. For f_k to represent an ultrashort pulse, Δk must be large enough, as will be demonstrated in the examples of Secs. V and VI below.

IV. THE VECTOR POTENTIAL

The vector potential amplitude $a(\rho,\zeta,\eta)$ may now be synthesized from the Fourier components $a_k(\rho,k,\eta)$ according to Eq. (3). In effect, one needs to evaluate

$$\begin{aligned} a(\rho,\zeta,\eta) &= \frac{1}{\sqrt{2\pi}} \int_{-\infty}^{\infty} \frac{f_k}{1+i\alpha_k} \exp\left[-\frac{\rho^2}{1+i\alpha_k}\right] e^{ik\zeta} dk, \\ &= \frac{1}{\Delta k} \int_{k_0-\Delta k/2}^{k_0+\Delta k/2} \psi_k e^{ik\zeta} dk, \end{aligned} \tag{8}$$

where

$$\psi_k = \frac{1}{1+i\alpha_k} \exp\left[-\frac{\rho^2}{1+i\alpha_k}\right]. \tag{9}$$

The remaining integrations in Eq. (8) can be very difficult to carry out analytically, so resorting to some well-known textbook transformations is inevitable. In brief, ψ_k will be viewed as a function of the combination $k + k_0 \equiv k'$ and then power series expanded about the central wave number k_0. Formally, this is done along the following lines:

$$\begin{aligned} \psi_k &= \sum_{m=0}^{\infty} \left.\frac{\partial^m \psi_k}{\partial k'^m}\right|_{k'=k_0} \frac{(k'-k_0)^m}{m!}, \\ &= \sum_{m=0}^{\infty} \psi_0^{(m)} \frac{k^m}{m!}; \quad \psi_0^{(m)}(\rho,\eta) \equiv \left.\frac{\partial^m \psi_k}{\partial k^m}\right|_{k=0}. \end{aligned} \tag{10}$$

Now, using Eqs. (8)–(10) in Eq. (2) gives

$$A(\rho,\zeta,\eta) = \frac{a_0 e^{ik_0\zeta}}{\Delta k} \sum_{m=0}^{\infty} \frac{\psi_0^{(m)}(\rho,\eta)}{m!} \int_{k_0-\Delta k/2}^{k_0+\Delta k/2} k^m e^{ik\zeta} dk. \tag{11}$$

The remaining integrations may be carried out one order at a time. For example, the *zeroth-order* fields may be obtained from the vector potential which follows from evaluation of the integral corresponding to $m = 0$, the *first-order* fields from the integral which involves terms up to the one labeled by $m = 1$, and so on. On the other hand, coefficients of the various powers of k in the power-series expansion (10) can, in principle, be evaluated to any desired order. Following are the first four such coefficients:

$$\psi_0^{(0)} = \frac{1}{P} \exp\left[-\frac{\rho^2}{P}\right]; \quad \psi_0^{(1)} = \frac{i\alpha}{k_0}\left[\frac{1}{P} - \frac{\rho^2}{P^2}\right]\psi_0^{(0)}, \tag{12}$$

$$\psi_0^{(2)} = \frac{i\alpha}{k_0^2}\left[-\frac{2(1+\rho^2)}{P^2} + \frac{\rho^2(4+\rho^2)}{P^3} - \frac{\rho^4}{P^4}\right]\psi_0^{(0)}, \tag{13}$$

$$\begin{aligned} \psi_0^{(3)} = \frac{i\alpha}{k_0^3}\Bigg[&\frac{3(2+4\rho^2+\rho^4)}{P^3} - \frac{\rho^2(18+12\rho^2+\rho^4)}{P^4} \\ &+ \frac{\rho^4(9+2\rho^2)}{P^5} - \frac{\rho^6}{P^6}\Bigg]\psi_0^{(0)}. \end{aligned} \tag{14}$$

In Eqs. (12)–(14)

$$P = 1 + i\alpha, \quad \alpha = \frac{\eta}{z_r}, \quad z_r = \frac{1}{2}k_0 w_0^2. \tag{15}$$

Recall that z_r is the depth of focus, otherwise known as the Rayleigh length, of the corresponding Gaussian beam. Up to

order n, Eq. (11) may now be written as

$$A^{(n)}(\rho,\zeta,\eta) = \frac{a_0 e^{ik_0\zeta}}{\Delta k}\sum_{m=0}^{n}\frac{\psi_0^{(m)}}{m!}S_m, \tag{16}$$

in which

$$S_m(\zeta) = \int_{k_0-\Delta k/2}^{k_0+\Delta k/2} k^m e^{ik\zeta}dk. \tag{17}$$

These integrals can readily be carried out, to give

$$S_0 = \frac{2e^{ik_0\zeta}}{\zeta}\sin\left(\frac{\zeta\Delta k}{2}\right), \tag{18}$$

$$S_m = (-i)^m\frac{\partial^m S_0}{\partial\zeta^m}. \tag{19}$$

With these equations at our disposal, analytic expressions can now, in principle, be obtained for the vector potential of the ultrashort, tightly focused laser pulse to any desired order. Before that is done, however, a small digression will be made here to comment on the convergence of the series (11). Unfortunately, convergence of this series is not manifestly guaranteed. Introducing a dimensionless variable u by letting $k = k_0 + u\Delta k$ transforms Eq. (8) into

$$a = e^{ik_0\zeta}\int_{-\frac{1}{2}}^{\frac{1}{2}}\psi_u e^{i\zeta(\Delta k)u}du, \tag{20}$$

where $\psi_u = \psi_k(k = k_0 + u\Delta k)$. Now, a series expansion of ψ_u about $u = 0$ turns (20) into

$$a = e^{ik_0\zeta}\sum_{m=0}^{\infty}\frac{(\Delta k)^m}{m!}\frac{\partial^m\psi_u}{\partial u^m}\int_{-\frac{1}{2}}^{\frac{1}{2}}u^m e^{i\zeta(\Delta k)u}du. \tag{21}$$

With $|u| \leqslant 1/2$, successive terms in the series tend to decrease, unless the derivatives of ψ_u increase with increasing order. The first few such derivatives are related to the ones given explicitly in Eqs. (12)–(14), which show that $\psi_0^{(m+1)}/\psi_0^{(m)} \sim 1/k_0$. The issue of convergence will be alluded to further, albeit numerically, at the end of Sec. V.

V. THE ZEROTH-ORDER VECTOR POTENTIAL

Adopting the initial axial envelope given by Eq. (7), the zeroth-order vector potential, according to Eq. (16), may be written as

$$A^{(0)} = a_0\frac{\exp\left[-\frac{\rho^2}{1+i\alpha}\right]}{1+i\alpha}e^{2ik_0\zeta}\frac{\sin(\zeta\Delta k/2)}{\zeta\Delta k/2},$$

$$= A_0\frac{\exp\left[-\frac{\rho^2}{1+\alpha^2}\right]}{\sqrt{1+\alpha^2}}\frac{\sin(\zeta\Delta k/2)}{\zeta\Delta k/2}e^{i\varphi^{(0)}}, \tag{22}$$

where

$$\varphi^{(0)} = \varphi_0 - \tan^{-1}\alpha + 2k_0\zeta + \frac{\alpha\rho^2}{1+\alpha^2}, \tag{23}$$

$$a_0 = A_0 e^{i\varphi_0};\quad \varphi_0 = \text{constant}. \tag{24}$$

Based on Eq. (22) the quantity $I^{(0)} \equiv |A^{(0)}|^2$, or

$$I^{(0)} = \frac{I_0}{1+\alpha^2}\exp\left[-\frac{2\rho^2}{1+\alpha^2}\right]\left[\frac{\sin(\zeta\Delta k/2)}{\zeta\Delta k/2}\right]^2, \tag{25}$$

may be considered an appropriate measure of the zeroth-order intensity, in which $I_0 = A_0^2$ is to be taken as the *initial* peak intensity at the pulse focus ($\rho = \zeta = \eta = 0$). Strictly speaking, the peak intensity is related to the square of the electric field amplitude $E_0 \sim \omega A_0$. However, we will continue referring to $|A^{(0)}|^2$ as *an intensity*, following Ref. [23]. The intensity profile is obviously a Gaussian in the transverse dimensions and has zeros along the axial direction at points corresponding to $\zeta\Delta k = \pm 2N\pi, N = 1,2,3,\ldots$. As has already been pointed out above, it makes sense to adopt $L = 2\pi/\Delta k$ as a measure of the initial ($t = 0$) axial length of the pulse. At any later time $t > 0$ the axial length $L(\zeta) \sim \Delta\zeta$ may be taken as the full width at half-maximum of the *instantaneous* axial intensity profile.

For the sake of better intuitive understanding, the zeroth-order intensity profile will, henceforth, be expressed explicitly in terms of the initial axial pulse length, L. This will cast the zeroth-order intensity into the following form:

$$I^{(0)} = \frac{I_0}{1+\alpha^2}\exp\left[-\frac{2\rho^2}{1+\alpha^2}\right]\left[\frac{\sin(\pi\zeta/L)}{\pi\zeta/L}\right]^2. \tag{26}$$

The main objective of this work, namely, to appropriately model the electric and magnetic fields of an ultrashort tightly focused laser pulse, has not yet been accomplished. Further insight will be gained from considering some limiting forms of the initial pulse intensity $I^{(0)}$. At $t = 0$, one has $\zeta = z, \eta = z/2, \alpha = z/(2z_r) = \lambda_0 z/(2\pi w_0^2)$, and the following *mathematical* limits may easily be evaluated. First,

$$\lim_{z\to 0} I^{(0)} = I_0 e^{-2\rho^2} \tag{27}$$

clearly exhibits the Gaussian nature of the initial intensity profile in the transverse coordinate ρ on the focal plane, $z = 0$. Second, for a long pulse

$$\lim_{L\to\infty} I^{(0)} = \frac{I_0}{1+(z/2z_r)^2}\exp\left[-\frac{2\rho^2}{1+(z/2z_r)^2}\right], \tag{28}$$

the intensity falls down on the propagation axis ($\rho = 0$) to 80% of its peak value at $z = \pm z_r$, to 50% at $z = \pm 2z_r$, and so on.

On the other hand, let us think of the pulse, for a moment, as containing a fixed number of photons per unit volume. With the intensity defined as energy crossing a unit area per unit time, this leads to the conclusion that $I^{(0)}$ is proportional to L, which is roughly the case according to Eq. (26). Therefore,

$$\lim_{L\to 0} I^{(0)} = 0 \tag{29}$$

is quite plausible.

The *mathematical* limits considered so far seem to suggest that our model should work well in representing the fields of a long pulse, for which $L \gg z_r$, as well as an ultrashort one ($L \ll z_r$). For a tightly focused pulse, behavior of the intensity at extreme values of the waist radius at focus, w_0, ought to be considered. For example, $I^{(0)} = I_0\exp[-2r^2/w_0^2]$ in the focal plane, $z = 0$. This quantity vanishes in the limit of $w_0 \to 0$ and reduces to I_0 as $w_0 \to \infty$.

The limits calculated above shed some light on the initial intensity profile and demonstrate that the intensity expression arrived at is well behaved mathematically. They are not entirely

conclusive about the general validity of the adopted model, or specifically in scenarios involving a pulse that is both tightly focused and ultrashort. For further insight, we resort to numerical calculations and include terms in the vector potential of order up to $n = 3$.

In Fig. 1, intensity profiles are shown which have been calculated at $t = 0$ from Eq. (26) and like expressions involving higher-order terms. The aim of this figure is twofold. On the one hand, it highlights the need, if at all, to go beyond the zeroth-order potential terms in modeling the fields appropriately. On the other hand, the figure helps us to understand what happens to the intensity as the pulse is focused tightly ($w_0 < \lambda_0$) and made ultrashort ($L < \lambda_0$). In Fig. 1(a), the waist radius at focus is $w_0 = 2\lambda_0$ and the axial pulse length is $L = 2\lambda_0$. These parameter values do not fit our definitions of *tightly focused* and *ultrashort*. For this parameter set, the terms in the fields above the zeroth-order term do not modify the intensity profile in any noticeable way. In Fig. 1(b), $w_0 = 2\lambda_0$, the same as in Fig. 1(a), but $L = 0.6\lambda_0$. A pulse with these parameters may be considered *ultrashort* but not necessarily *tightly focused*. Here, too, there appears to be no need to include terms in the model of order higher than the lowest. Recall that an axially short pulse has a broad frequency spectrum, according to the relation $\Delta k = 2\pi/L$. In Fig. 1(a), $\Delta k = k_0/2$, whereas it is $\Delta k = 5k_0/3$ in Fig. 1(b). Hence, the change in axial pulse length from Fig. 1(a) to Fig. 1(b). Figure 1(c) displays the intensity profile of a *tightly focused* pulse ($w_0 = 0.6\lambda_0$) that is not necessarily *ultrashort* ($L = 2\lambda_0$). Its frequency spectrum is as broad as that of Fig. 1(a), which is consistent with the fact that it has the same axial length. Inclusion, in this particular case, of every term of order $n \leqslant 3$ seems to alter the intensity profile slightly, and sometimes even drastically when terms of order $n > 3$ are employed.

The intensity profile of a pulse that is both *tightly focused* and *ultrashort* ($w_0 = L = 0.6\lambda_0$) is shown in Fig. 1(d). It is quite remarkable that, for these parameters, inclusion of terms in the description of the fields, beyond what may be obtained from the zeroth-order vector potential alone, does not alter the intensity profile appreciably. Modification to the central part of the profile is negligibly small, while the side lobes are altered more significantly.

In some publications [23], *ultrashort* is defined in terms of the axial length as it compares with the Rayleigh length $z_r = k_0 w_0^2/2$. Within this context, an ultrashort pulse is one for which $L \ll z_r$. The cases considered in Figs. 1(a)–1(d) correspond to $L/z_r \sim 0.159, 0.159, 0.531$, and 0.531, respectively. All cases, for which Fig. 1 displays the intensity profile, may thus be considered ultrashort.

Figure 2 focuses on the case considered in Fig. 1(d) ($w_0 = L = 0.6\lambda_0, z_r \sim 0.531\lambda_0$) at $t = 0$ and at later times ($t = 1$ fs and 1 ps). The centroid of the pulse, which initially (at $t = 0$) is at $z = 0$, as depicted in Fig. 1(d), is shown to advance to $z = ct = 0.3\lambda_0$ and $300\lambda_0$, according to Figs. 2(a) and 2(b), respectively. Note that the need to include terms in the vector potential beyond those of $n = 3$ does not arise in Fig. 2(b) before what may be considered *convergence* is achieved. Calculations, whose results are not shown here, lead to the conclusion that the convergence remains robust even after terms of order $n = 8$ have been included.

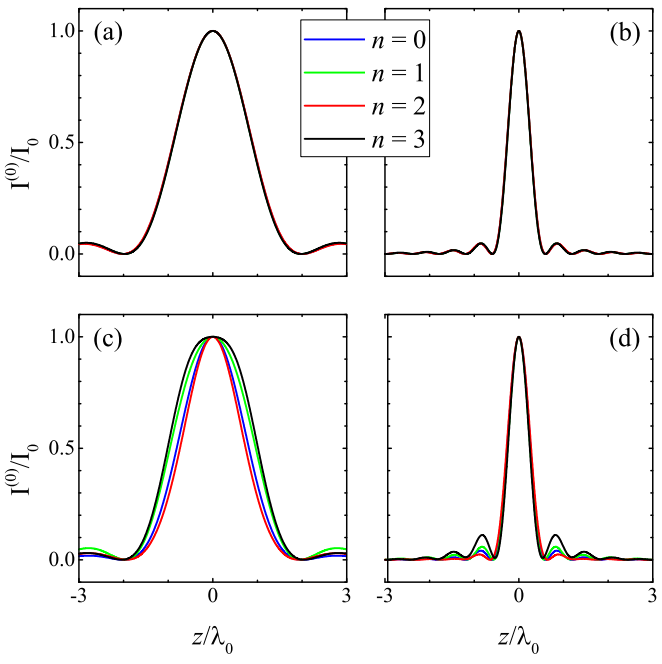

FIG. 1. (Color online) Variation of the initial (at $t = 0$) normalized intensity with distance along the propagation direction, at points on the axis of propagation ($x = 0 = y$) of pulses for which (a) $w_0 = L = 2\lambda_0$, (b) $w_0 = 2\lambda_0$ and $L = 0.6\lambda_0$, (c) $w_0 = 0.6\lambda_0$ and $L = 2\lambda_0$, and (d) $w_0 = L = 0.6\lambda_0$. Note that $w_0 = 2\lambda_0$ and $0.6\lambda_0$ correspond to the Rayleigh lengths $z_r \sim 12.57\lambda_0$ and $1.13\lambda_0$, respectively. To produce each panel of figures, fields to orders $n = 0$–3 have been employed.

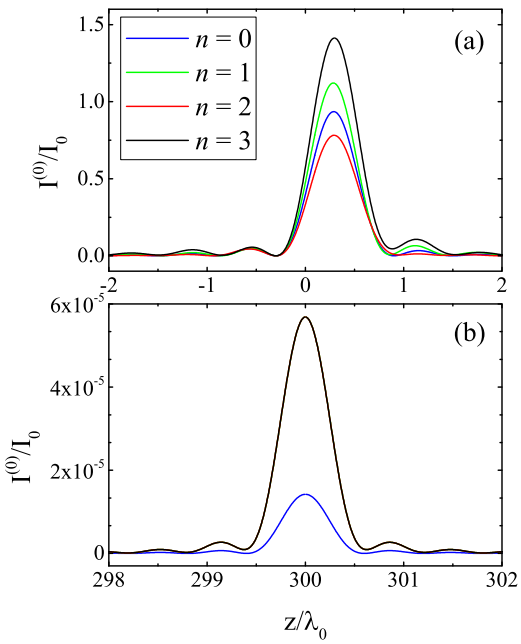

FIG. 2. (Color online) Snapshots of the normalized intensity along the propagation direction, at points on the axis of propagation ($x = 0 = y$) of pulses for which $w_0 = L = 0.6\lambda_0$, taken at (a) $t = 1$ fs and (b) $t = 1$ ps. To produce each panel of figures, fields to orders $n = 0$–3 have been employed.

VI. THE ELECTRIC AND MAGNETIC FIELDS

The discussion of Fig. 1 leads to the conclusion that the zeroth-order vector potential does model an ultrashort, tightly focused, pulse quite well. Therefore, this section is devoted to analytic derivation of the electric and magnetic fields to zeroth order only. Expressions for the higher order corrections may, in principle, be found following the program outlined here and in Sec. IV.

The electric and magnetic fields will be obtained from the vector and scalar potentials, via the equations [26]

$$\boldsymbol{E} = -\frac{\partial \boldsymbol{A}}{\partial t} - \boldsymbol{\nabla}\Phi \quad \text{and} \quad \boldsymbol{B} = \boldsymbol{\nabla} \times \boldsymbol{A}. \tag{30}$$

Since the wave equations satisfied by Φ and A_z are identical, they must have identical formal solutions, apart from a multiplicative constant to make the units right. Using the ansatz (2) for the vector potential, the general structure of the scalar potential must be the same, namely, $\Phi = \phi_0\phi(x,y,z,t)\exp(ik_0\zeta)$. Thus, one has

$$\begin{aligned}\frac{\partial \Phi}{\partial t} &= \phi_0\left(\frac{\partial \phi}{\partial t} - ick_0\phi\right)e^{ik_0\zeta},\\ &= \left(\frac{1}{\phi}\frac{\partial \phi}{\partial t} - ick_0\right)\Phi,\\ &= \left(\frac{1}{a}\frac{\partial a}{\partial t} - ick_0\right)\Phi.\end{aligned} \tag{31}$$

In the last line of Eq. (31), the assertion made above that the equations satisfied by the two potentials have identical solutions has been used. Now, the Lorenz condition

$$\boldsymbol{\nabla}\cdot\boldsymbol{A} + \frac{1}{c^2}\frac{\partial \Phi}{\partial t} = 0 \tag{32}$$

gives

$$\Phi = \frac{c^2}{R}(\boldsymbol{\nabla}\cdot\boldsymbol{A}); \quad R = ick_0 - \frac{1}{a}\frac{\partial a}{\partial t}. \tag{33}$$

Then, the first of Eq. (30) yields

$$\boldsymbol{E} = -\frac{\partial \boldsymbol{A}}{\partial t} - \frac{c^2}{R}\boldsymbol{\nabla}(\boldsymbol{\nabla}\cdot\boldsymbol{A}) - \frac{c^2}{R^2}(\boldsymbol{\nabla}\cdot\boldsymbol{A})\boldsymbol{\nabla}\left(\frac{1}{a}\frac{\partial a}{\partial t}\right). \tag{34}$$

With $\boldsymbol{A}$ polarized in the axial (z) direction and employing cylindrical coordinates (r,θ,z) in this equation, the electric field will have radial and axial components, which follow individually from

$$E_r = -\frac{c^2}{R}\frac{\partial}{\partial r}\left(\frac{\partial A}{\partial z}\right) - \frac{c^2}{R^2}\left(\frac{\partial A}{\partial z}\right)\frac{\partial}{\partial r}\left(\frac{1}{a}\frac{\partial a}{\partial t}\right) \tag{35}$$

and

$$E_z = -\frac{\partial A}{\partial t} - \frac{c^2}{R}\frac{\partial^2 A}{\partial z^2} - \frac{c^2}{R^2}\left(\frac{\partial A}{\partial z}\right)\frac{\partial}{\partial z}\left(\frac{1}{a}\frac{\partial a}{\partial t}\right). \tag{36}$$

Note that the radial electric field, E_r, is entirely due to the scalar potential, the second and third terms in Eq. (34). Similarly, the second and third terms in the axial electric field, E_z, stem from the scalar potential. The magnetic field, on the other hand, will have only an azimuthal component, which may be obtained from

$$B_\theta = -\frac{\partial A}{\partial r}. \tag{37}$$

In principle, Eqs. (35)–(37) may be used to derive fully analytic expressions for the $\boldsymbol{E}$ and $\boldsymbol{B}$ fields of the pulse to any desired order, but with the expected rising complexity with increasing order. Some space will next be devoted to a discussion of the lowest-order fields, ones derived from the zeroth-order vector potential.

Keeping only the zeroth-order term in the vector potential, expressions may be found for the lowest-order terms in the fields. After some elaborate algebra, one gets

$$\begin{aligned}E_r^{(0)} = \frac{E_0}{k_0 w_0}\frac{\rho e^{-\rho^2/P}}{P^2}\frac{e^{2ik_0\zeta}}{\pi\zeta/L}\Bigg\{&\left[\frac{cQ_2}{R} - \frac{ic^2Q_3}{2z_rPR^2}\right]\\ &\times \sin\left(\frac{\pi\zeta}{L}\right) + \frac{2\pi}{L}\left[\frac{c}{R} - \frac{ic^2}{2z_rPR^2}\right]\cos\left(\frac{\pi\zeta}{L}\right)\Bigg\},\end{aligned} \tag{38}$$

$$\begin{aligned}E_z^{(0)} = \frac{E_0}{2k_0}\frac{e^{-\rho^2/P}}{P}\frac{e^{2ik_0\zeta}}{\pi\zeta/L}\Bigg\{&\left[Q_1 + \frac{cQ_4}{R} + \frac{c^2Q_3Q_5}{R^2}\right]\\ &\times \sin\left(\frac{\pi\zeta}{L}\right) + \frac{2\pi}{L}\left[1 - \frac{cQ_3}{R} + \frac{c^2Q_5}{R^2}\right]\cos\left(\frac{\pi\zeta}{L}\right)\Bigg\},\end{aligned} \tag{39}$$

$$cB_\theta^{(0)} = \frac{2E_0}{k_0 w_0}\frac{\rho e^{-\rho^2/P}}{P^2}\frac{e^{2ik_0\zeta}}{\pi\zeta/L}\sin\left(\frac{\pi\zeta}{L}\right). \tag{40}$$

The superscript (0) is added to emphasize that it is the zeroth-order fields that are considered here. The remaining terms in Eqs. (38)–(40) have the following definitions:

$$E_0 = ck_0a_0; \quad R = \frac{c}{2}\left[Q_1 + \frac{2\pi}{L}\cot\left(\frac{\pi\zeta}{L}\right)\right], \tag{41}$$

$$\begin{aligned}Q_1 &= 4ik_0 - \frac{2}{\zeta} + \frac{i(P-\rho^2)}{z_rP^2};\\ Q_2 &= 4ik_0 - \frac{2}{\zeta} - \frac{i(2P-\rho^2)}{z_rP^2};\\ Q_3 &= 4ik_0 - \frac{2}{\zeta} - \frac{i(P-\rho^2)}{z_rP^2},\end{aligned} \tag{42}$$

$$\begin{aligned}Q_4 = 8k_0^2 + \frac{2\pi^2}{L^2} + \frac{2Q_3}{\zeta}&\\ - \frac{4k_0(P-\rho^2)}{z_rP^2} + \frac{2P^2 - 4P\rho^2 + \rho^4}{2z_r^2P^4};&\\ Q_5 = \frac{1}{\zeta^2} + \frac{P-2\rho^2}{4z_r^2P^3} - \frac{\pi^2}{L^2}\csc^2\left(\frac{\pi\zeta}{L}\right).&\end{aligned} \tag{43}$$

Note that the radial electric field, $E_r^{(0)}$, and the *azimuthal* magnetic field, $B_\theta^{(0)}$, vanish identically on the propagation axis ($\rho = 0$). On the other hand, the axial component, $E_z^{(0)}$, is quite strong along the propagation axis, giving the fields the well-known pencil-like focus. These results are quite important for some applications, including particle laser acceleration [27] and material processing [1].

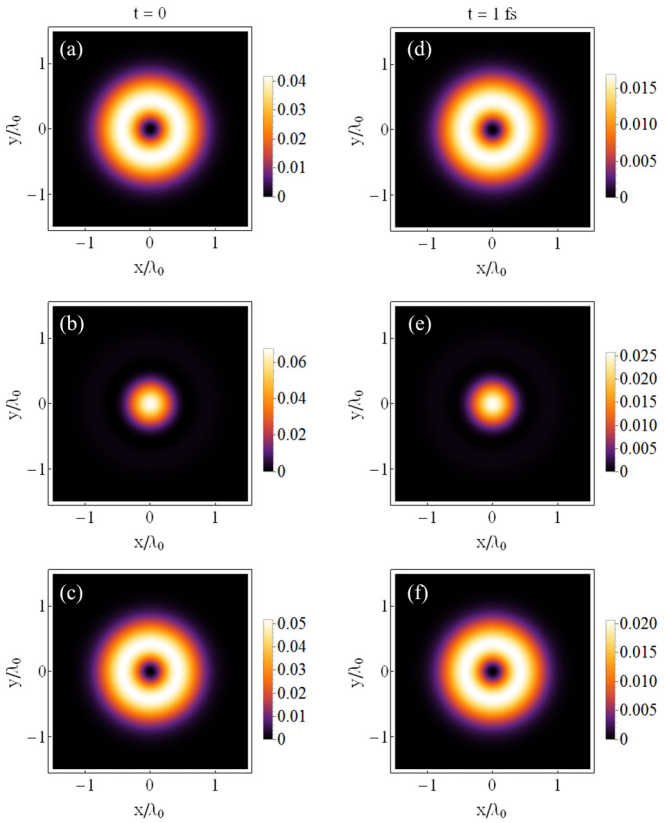

FIG. 3. (Color online) Density plots in the focal plane ($z = 0$) perpendicular to the propagation direction, of the normalized intensities. The panel on the left is for $t = 0$ and that on the right is for $t = 1$ fs. The plots are for a pulse with $w_0 = 0.6\lambda_0 = L$.

To further highlight the main characteristics of the radially polarized fields of an ultrashort and tightly focused laser pulse, density plots of the scaled intensities $|E_r^{(0)}/E_0|^2$,$|E_z^{(0)}/E_0|^2$, and $|cB_\theta^{(0)}/E_0|^2$ in the focal plane ($z = 0$) are shown in Fig. 3. Plots of the initial intensities (at $t = 0$) are displayed in Figs. 3(a)–3(c) and at $t = 1$ fs in Figs. 3(d)–3(f). First, note that the axial symmetry of the fields, and the vanishing of $E_r^{(0)}$ and $cB_\theta^{(0)}$ at points along the propagation axis, are reflected clearly in the density plots. Signature of the pencil-like focus is also reflected in the shape of the $|E_z^{(0)}/E_0|^2$ density plots, in that it peaks at the center ($x = y = 0$).

Not clearly exhibited in Fig. 3 are the relative strengths of the various fields. To bring that out, three-dimensional (3D) surface plots of the scaled intensities are shown in Fig. 4, employing the parameter set used in Fig. 3. As expected for a radially polarized pulse, the axial field strength E_z is stronger than that of the radial component E_r. Recall that Figs. 3 and 4 are *snapshots* at the time instants $t = 0$ and 1 fs. The initial fields produce global intensity maxima at $t = 0$. Subsequent evolution results in intensity profiles of lower height due to the oscillatory nature of the fields and the inevitable diffraction effects.

A minor issue related to the propagation characteristics of the pulse will finally be addressed here. Snapshots displaying the (spatial) variations (with the propagation distance, z) of the normalized intensity profile $|E_z^{(0)}/E_0|^2$ are shown in Fig. 5. Decrease in the maximum intensity is due to the diffraction

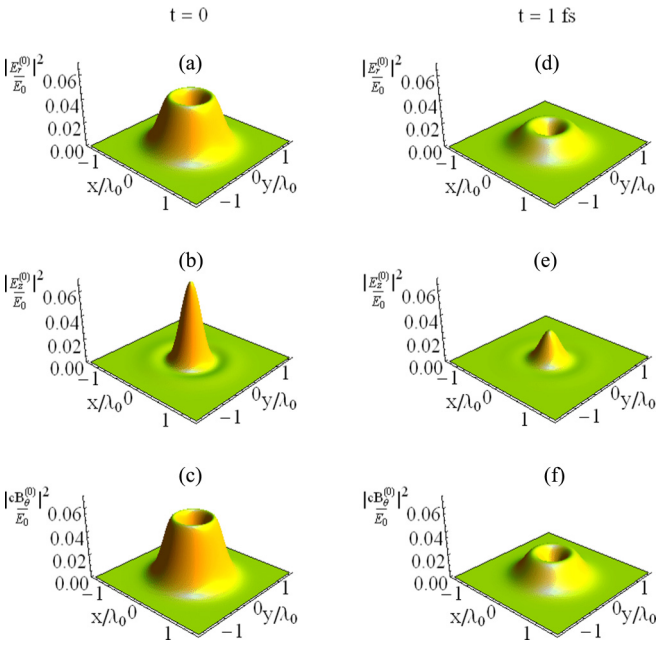

FIG. 4. (Color online) Variations in the focal plane ($z = 0$) of the normalized intensity distributions. Panel on the left is for $t = 0$ and that on the right is for $t = 1$ fs. All parameters are the same as in Fig. 3.

effects and the oscillatory nature of the fields, alluded to in the previous paragraph. Also, the centroid of the pulse is shown to advance along the propagation direction at roughly the speed of light, so its position is always given by $z \sim ct$. This behavior

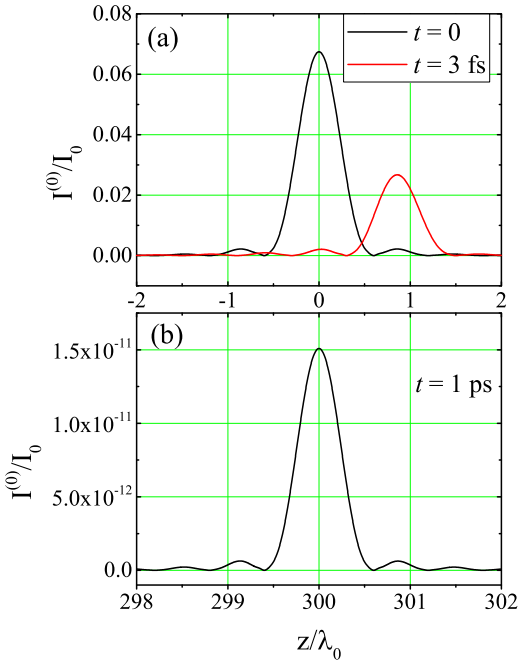

FIG. 5. (Color online) Variation of the normalized *axial* intensity with distance along the propagation direction, at points on the axis of propagation ($x = 0 = y$) of a pulse that is both ultrashort and tightly focused ($w_0 = L = 0.6\lambda_0$ and $z_r \sim 1.13\lambda_0$). Shown are snapshots at times $t = 0,3$ fs and 1 ps.

is consistent with what has been encountered in Fig. 2, which, it must be borne in mind, was based upon the *total* intensity (derived from the *full* vector potential).

VII. CONCLUSIONS

This paper has been devoted to the derivation of analytic expressions for the electric and magnetic fields of an ultrashort and tightly focused radially polarized laser pulse. A solution to the wave equation satisfied by the vector potential, polarized in the direction of propagation, has been the starting point for the derivation, which also brought into the picture a scalar potential via the Lorenz gauge. The procedure employed to arrive at the main results followed along lines similar to the work of Esarey *et al.* [23] (for a linearly polarized pulse) with two major differences. On the one hand, a scalar potential has been used here explicitly and throughout the derivation. This has resulted in expressions for the transverse as well as axial fields in a natural way. In Ref. [23] only a vector potential is used and it is suggested there that the axial electric field could be obtained via the Maxwell equation $\nabla \cdot \boldsymbol{E} = 0$. On the other hand, an intuitively clear and simple choice for the initial pulse profile in k space has been used in our work, instead of the Gaussian employed in Ref. [23]. This choice has resulted in a number of simplifications, which, in turn, led to straightforward integrals and to an intuitively clear interpretation of the final results.

Final field expressions have been derived only to lowest order, stemming from a power-series expansion which has been employed at some point in the derivation in order to facilitate analytic calculation of the otherwise quite involved inverse Fourier transform integrals. The derived field expressions have been used to produce the well-known donut-shaped intensity profiles of the radial electric and azimuthal magnetic fields, E_r and B_θ, respectively, as well as the equally well-known pencil-like focus of the axial electric field E_z. It has been demonstrated, via specific numerical examples, that the need to retain terms in the field expressions beyond the lowest order may not be necessary. Nevertheless, a program has been designed that would lead one to obtain analytic expressions for the fields to all desired orders. The main steps have been spelled out and most of the analytic work, needed to arrive at the vector potential, has been done.

[1] M. Meier, V. Romano, and T. Feurer, Appl. Phys. A **86**, 329 (2007).
[2] L. F. Li *et al.*, Appl. Phys. Lett. **105**, 221103 (2014).
[3] P. Li, S. Liu, G. F. Xie, T. Peng, and J. L. Zhao, Opt. Express **23**, 7131 (2015).
[4] H. Pu, J. Shu, Z. Chen, Z. Lin, and J. Pu, J. Opt. Soc. Am. A **32**, 1717 (2015).
[5] S. Roy, K. Ushakova, Q. van den Berg, S. F. Pereira, and H. P. Urbach, Phys. Rev. Lett. **114**, 103903 (2015).
[6] M.-D. Wei, Y.-S. Lai, and K.-C. Chang, Opt. Lett. **38**, 2443 (2013).
[7] C. Varin *et al.*, Apply. Sci. **3**, 70 (2013).
[8] P.-L. Fortin, M. Piché, and C. Varin, J. Phys. B: At. Mol. Opt. Phys. **43**, 025401 (2010).
[9] http://www.eli-beams.eu/.
[10] H. S. Ghotra and N. Kant, Opt. Commun. **356**, 118 (2015).
[11] J.-X. Li, Y. I. Salamin, B. J. Galow, and C. H. Keitel, Phys. Rev. A **85**, 063832 (2012).
[12] Y. I. Salamin, Phys. Lett. A **374**, 4950 (2010).
[13] S. Payeur, S. Fourmaux, B. E. Schmidt, J. P. MacLean, C. Tchervenkov, F. Légaré, M. Piché, and J. C. Kieffer, Appl. Phys. Lett. **101**, 041105 (2012).
[14] R. Dorn, S. Quabis, and G. Leuchs, Phys. Rev. Lett. **91**, 233901 (2003).
[15] Z. Cheng, Y. Y. Zhou, M. Xia, W. Li, K. C. Yang, and Y. F. Zhou, Opt. Las. Tech. **73**, 77 (2015).
[16] Y. I. Salamin, Phys. Rev. A **82**, 013823 (2010).
[17] Y. I. Salamin, New J. Phys. **8**, 133 (2006).
[18] Y. I. Salamin, Opt. Lett. **31**, 2619 (2006).
[19] C. Varin, M. Piché, and M. A. Porras, JOSA A **23**, 2027 (2006).
[20] Q. Lin, J. Zheng, and W. Becker, Phys. Rev. Lett. **97**, 253902 (2006).
[21] A. April, Opt. Lett. **33**, 1392 (2008).
[22] A. April, Opt. Lett. **33**, 1563 (2008).
[23] E. Esarey, P. Sprangle, M. Pilloff, and J. Krall, J. Opt. Soc. Am. B **12**, 1695 (1995).
[24] http://puhep1.princeton.edu/~kirkmcd/examples/axicon.pdf.
[25] J.-X. Li, Y. I. Salamin, K. Z. Hatsagortsyan, and C. H. Keitel, arXiv:1504.00988.
[26] J. D. Jackson, *Classical Electrodynamics*, 3rd edition (Wiley, New York, 1998).
[27] Y. I. Salamin, Phys. Lett. A **375**, 795 (2011).